Environmental Science and Pollution Research (2021) 28:10633–10641
https://doi.org/10.1007/s11356-020-11340-8

RESEARCH ARTICLE

New catalyst comprising Silicotungstic acid and MCM-22 for degradation of some organic dyes

Dhruvi Pithadia[1] · Vinayak Hegde[2] · Varsha P. Brahmkhatri[2] · Anjali Patel[1]

Received: 21 June 2020 / Accepted: 20 October 2020 / Published online: 24 October 2020

Abstract

A heterogeneous catalyst comprising Keggin type polyoxometalate, silicotungstic acid (SiW_{12}), and MCM-22 was synthesized using wet impregnation method and characterized by acidity measurement, BET, FT-IR, XRD, and SEM. Their catalytic activity was evaluated for the degradation of cationic organic dyes like methylene blue (MB), crystal violet (CV), and an azo dye Chryosidine Y (CY) in an aqueous solution. The experimental parameters such as catalyst amount, initial dye concentration, and contact time were studied for the degradation of dyes, and it was found that the cationic dyes like methylene blue and crystal violet show better activity as compared to azo dye Chryosidine Y. This may be attributed to better electrostatic interaction of these cationic dyes with the residual negative surface charge of the catalyst, due to presence of SiW_{12} ion as it is rich in surface oxygens and surface hydroxyl groups. The control experimental results showed that the presence of SiW_{12} at the surface of MCM-22 promoted the degradation reactions, and presence of multiple W–O bonds in polyoxometalate also played a key role in this reaction. The catalyst exhibits recycling ability without any significant loss in activity up to four cycles.

Keywords Silicotungstic acid · MCM-22 · Heterogeneous catalyst · Dye degradation · Multiple dyes

Introduction

Dyes are primarily used in paints, textiles, printing inks, paper, and plastics that are majorly associated with textile industry (Yaseen and Scholz 2019; Berradi et al. 2019). The natural dyes were replaced by chemical dyes that can bind to the fabric for longer time and retain colour throughout washing and exposure. The chemical dyes are generally soluble and organic in nature. They are classified as reactive, direct, basic, and acidic dyes (Benkhaya et al. 2020). They exhibit high solubility in water making it difficult to remove them by conventional methods. One of its properties is the ability to impart colour to a given substrate, because of the presence of chromophoric groups in its molecular structure (Gürses et al. 2016). However, the property of fixing the colour to the material is related to the polar auxotrophic groups that can bind to polar groups of textile fibres. Exposure to dye-bearing wastewater exhibits severe harmful effect causing an environmental pollution, and it is also associated with health hazards as the degradation products of dyes are carcinogenic in nature (Tkaczyk et al. 2020; Lellis et al. 2019). Due to the adverse effects of dye effluents on environment and health, legislation on the limits of colour discharge by industrial activities has become increasingly strict by the authorities, and treatment of dye water is mandatory before submerging it with natural water bodies (Asolekar et al. 2014).

There are mainly three ways to remove the dyes from polluted water bodies: physical, chemical, and biological methods (Hayat et al. 2015). Many techniques under these categories like reverse osmosis (Wang et al. 2018), electrochemical coagulation (Aragaw 2020), nanofiltration (Khumalo et al. 2019), adsorption (Kumari et al. 2020), oxidation (Dadashi Firouzjaei et al. 2020), electrocatalysis (Singh et al. 2013), and degradation by enzymes and microorganisms (Vikrant et al. 2018) have been explored for the removal of

Dhruvi Pithadia and Vinayak Hegde contributed equally to this work.

Responsible Editor: Santiago V. Luis

✉ Varsha P. Brahmkhatri
b.varsha@jainuniversity.ac.in

✉ Anjali Patel
anjali.patel-chem@msubaroda.ac.in

[1] Polyoxometalates and Catalysis Laboratory, Department of Chemistry, Faculty of Science, The Maharaja Sayajirao University of Baroda, Vadodara, Gujarat 390002, India

[2] Centre for Nano and Material Sciences, Jain University, Jain Global Campus, Bengaluru, Karnataka 562112, India

Table 1 Textural properties and acidity measurement of support and catalysts

Material	Total acidity (mmol g^{-1})	BET surface area (m^2/g)
MCM-22	0.86	267
$(SiW_{12})_1$/MCM-22	0.99	-
$(SiW_{12})_2$/MCM-22	1.11	-
$(SiW_{12})_3$/MCM-22	1.22	234
$(SiW_{12})_4$/MCM-22	1.3	230

dye from wastewater (Han et al. 2016). For the treatment of dye wastewater, it is important to remove dyes and their degradation by oxidation or by catalytic processes.

Polyoxometalate (POM)-based heterogeneous catalysts (Narkhede et al. 2015; Patel and Pathan 2015) are gaining interest in environmental remediation processes including water treatment (Sivakumar et al. 2012; Herrmann et al. 2017). The reports suggest that POM-based materials are coming up as emerging catalyst for dye degradation studies for environmental remediation of dye contaminated water. For example, in an earlier report on resin-supported POMs, parent ($PW_{12}O_{40}^{3-}$) and its lacunary derivative ($PW_{11}O_{39}^{7-}$) were found to catalyse the degradation and partial mineralization of cationic dye pollutants in the presence of H_2O_2 using visible light irradiation (Lei and Chen 2005). In another report, the La^{3+} and Ce^{3+} loaded $H_3PW_{12}O_{40}$ catalysts were explored for photodegradation of methyl orange and rhodamin B under UV and visible light irradiation (Li et al. 2014). With further alterations, an immobilized phosphotungstic acid with zeolite (SBA-15)-modified BiOBr composites was investigated for photocatalytic degradation of methyl orange (Wang et al. 2017). Another catalyst comprising of $H_3PMo_2W_{10}O_{40}$ and $H_3PMo_4W_8O_{40}$@ethylene diamin functionalized magnetic graphene was reported for removal of methylene blue dye (Fakhri et al. 2017). Recently, substituted Keggin type polyoxometalate/hydrotalcites with Mn and Fe were reported for degradation of multiple dyes (Wu et al. 2020). Along with such modifications, report on the utilization of two inorganic-organic hybrid materials based on octamolybdate for wet air oxidation of Bismarck brown (BB), Azure II, Direct blue 71 (DB 71), methyl violet (MV), and methylene blue (MB) showed efficient catalytic degradation activity under mild conditions (Najafi et al. 2015). A new hybrid material comprising POM and metal organic framework (MOFs) $\{[(Cu_4Cl)(CPT)_4]\cdot(HSiW_{12}O_{40})\cdot 31H_2O$ was fabricated and tested for rhodamine B degradation studies (Chen et al. 2018). Another composite catalyst based on POM ($K_6P_2W_{18}O_{62}$ polyoxometalate) encapsulated into mesoporous UiO-66 metal organic framework was reported for degradation of cationic dyes rhodamine B (RhB) and malachite green (MG) and one anionic dye orange G (Zeng et al. 2018). Apart from Keggin type, report on a study of a Dawson heteropoly acid, chemically anchored to the amine-functionalized nanosilica and its photocatalytic degradation efficiency, was explored for an aqueous solution of malachite green (Bamoharram et al. 2014). Also, a nano-POM composite consisting of saturated Dawson anions ($\alpha_2P_2W_{17}CoO_{61}$) was reported for degradation of azo dyes (Grabsi et al. 2019). Likewise, another type of an organic-inorganic hybrid Lindqvist-type polyoxometalate (POM) anions, $\{W_6O_{19}\}^{2-}$, and cucurbituril based photocatalyst was also found to be active for degradation of rhodamine B (Cao et al. 2017).

Above literature survey shows that no reports are available for the utilization of modified zeolites, especially MCM-22, via Keggin type POM, i.e. SiW_{12}, for the degradation of cationic dyes. In present study, for first time, we are reporting the synthesis of a new catalyst, comprising MCM-22 and SiW_{12} for the dye degradation study. The synthesized catalyst was characterized by various physicochemical techniques, and catalytic degradation study was carried out for cationic dyes like methylene blue (MB), crystal violet (CV), and an azo dye

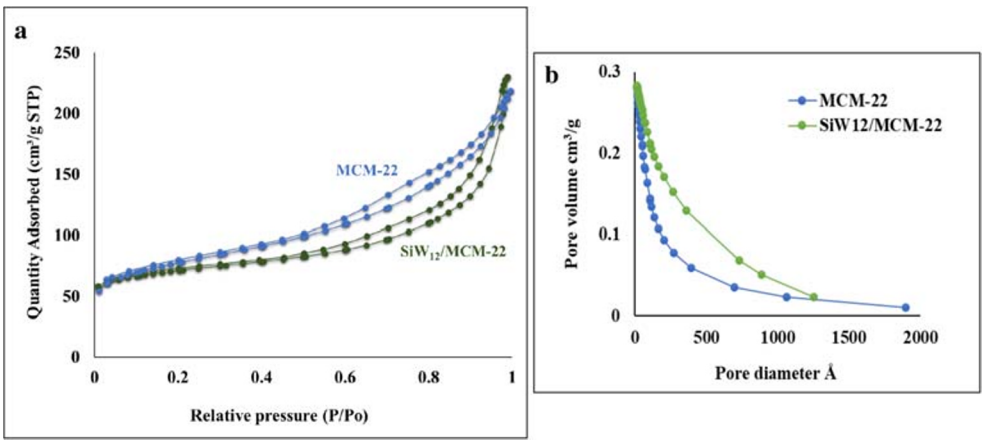

Fig. 1 (**a**) N_2 adsorption-desorption isotherms and (**b**) BJH pore size distribution

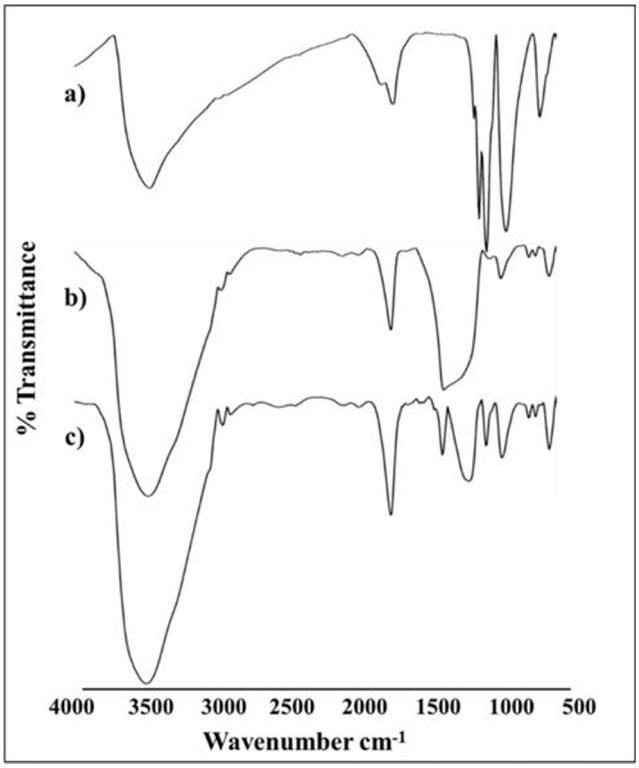

Fig. 2 FT-IR spectra of (**a**) SiW_{12}, (**b**) MCM-22, and (**c**) SiW_{12}/MCM-22

Chryosidine Y (CY). We have investigated various reaction parameters like dye concentration, catalyst amount, and reaction time for the same, and the results demonstrated that the present catalyst could be used for the removal of various dyes from water. The catalyst was recycled up to four cycles of reaction, which indicates the reusability and stability of the catalysts.

Materials and methods

Materials

All chemicals used were of A.R. grade. Silicotungstic acid was used as received from Merck. MCM-22 was acquired commercially from BEE CHEMS (Kanpur, UP). All the three dyes, methylene blue, crystal violet, and an azo dye Chryosidine Y, were received from Nice Chemicals Pvt. Ltd (Bangalore).

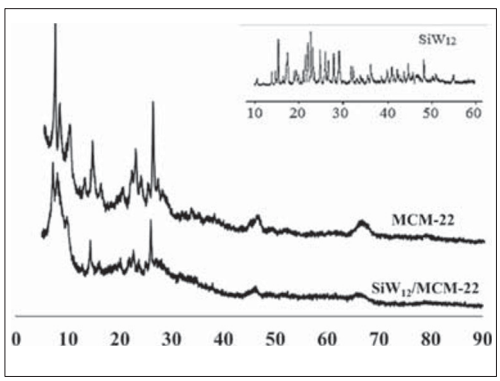

Fig. 3 Powder XRD of support and catalyst

Synthesis of the catalyst (SiW_{12} anchored to MCM-22)

A series of catalysts comprising 10–40% of SiW_{12} anchored to MCM-22 was synthesized by wet impregnation method. Impregnation was carried out by adding 1 g of MCM-22 into aqueous solution of SiW_{12} (0.1 g/10 mL–0.4 g/ 40 ml of distilled water), and the resulting suspension was dried at 100 °C for 10 h. The obtained catalysts were designated as $(SiW_{12})_1$/MCM-22, $(SiW_{12})_2$/MCM-22, $(SiW_{12})_3$/MCM-22, and $(SiW_{12})_4$/MCM-22, respectively.

Characterization

Determination of total acidity by n-butylamine titration method

Total acidity of support and catalyst were determined by performing n-butylamine titration. In 25 ml 0.025 N n-butylamine solution (in toluene), 0.25 g of support/catalyst was suspended and allowed to neutralize for 24 h. Total acidity of support/catalyst was obtained by titrating remaining base against 0.025 N trichloroacetic acid solution in toluene using neutral red indicator.

Physicochemical techniques

BET surface area measurements were carried out in a Micromeritics ASAP 2010 volumetric static adsorption instrument using N_2 adsorption at 77 K and by BJH adsorption-desorption method, and the pore size distributions were calculated. FT-IR analysis was carried out by compelling the solid samples into discs with dry KBr and recorded in the range of 4000–400 cm^{-1} (wave numbers) using Shimadzu instrument (IRAffinity-1S). For X-ray powder diffraction (XRD) patterns, samples were analysed in the 2θ range of 5–90° (CuKα radiation λ = 1.54056 Å) using Philips X′ pert MPD system. Scanning electron microscope (SEM) images were recorded with JSM-7100F scanning electron microscope.

Catalytic activity test

The performance of SiW_{12}/MCM-22 was tested for the degradation of multiple dyes like MB, CV, and CY at room temperature, 28 °C. At regular time intervals, 2 ml of the mixture was taken out from the reaction mixture and filtrated by using a 0.22-μm syringe filter in order to

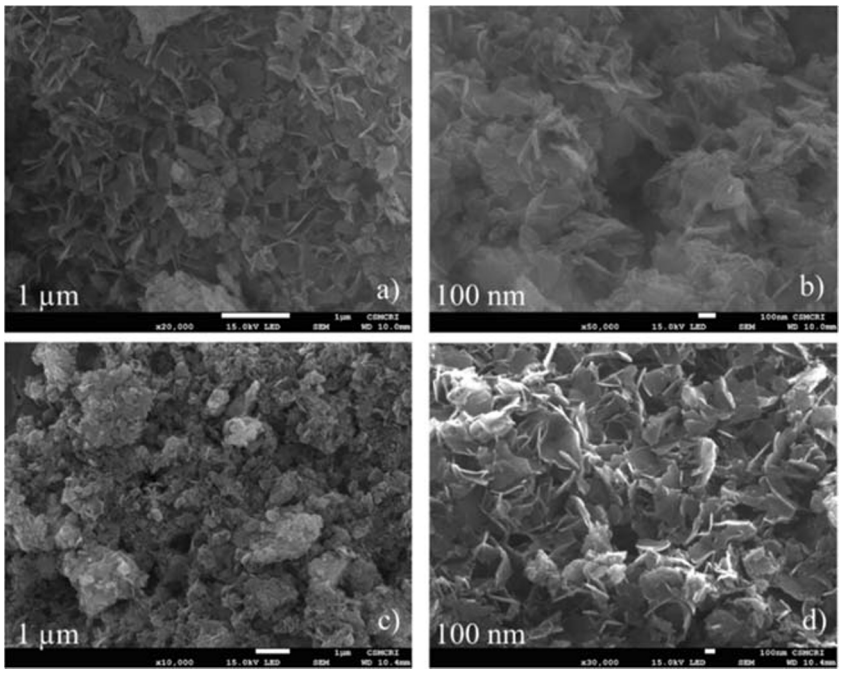

Fig. 4 SEM images of (**a**, **b**) MCM-22 and (**c**, **d**) SiW_{12}/MCM-22

completely remove catalyst particles. The dye concentration in the solution was measured by UV-visible spectrophotometer (ShimadzuUV-1800) at the maximum adsorption wavelength of dye. For recyclability experiments, the catalyst was centrifuged, washed with water, and dried at 60 °C. The following equation was used to calculate dye degradation efficiency.

$$\text{Degradation efficiency}\ (\%) = (C_0{-}C)/C_0 \times 100\%$$

where C_0 was the initial dye concentration and C was the dye at certain concentration time t during the reaction.

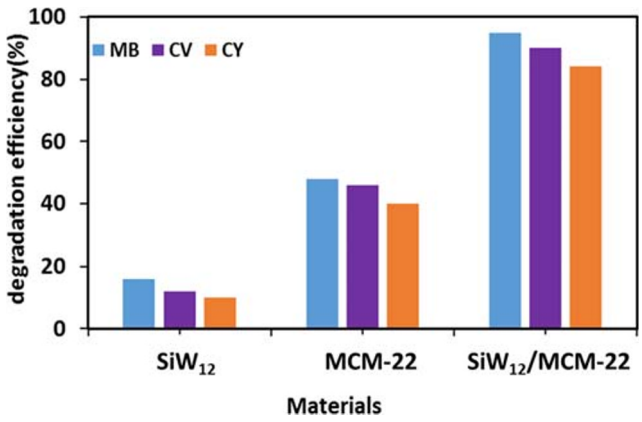

Fig. 5 Control experiments, degradation efficiency of MCM-22, SiW_{12}, and catalyst SiW_{12}/MCM-22. Reaction conditions: dye concentration, 100 ppm; amount of materials taken MCM-22 = 20 mg/mL, SiW_{12}, 1 mg/ml; reaction time, 60 min

Results and discussion

Characterization of catalyst

Textural properties of support and catalyst are shown in Table 1. BET surface area of SiW_{12}/MCM-22 is lower as compared to that of MCM-22, which is the first indication of the incorporation of SiW_{12} species inside the zeolitic pores of MCM-22. From the values of total acidity of support as well as catalysts (Table 1) obtained by n-butylamine titration, it is observed that as the amount of SiW_{12} increases, acidity increases due to the increase in Bronsted acidic sites. Substantial increase in total acidity is observed from 10 to 30% loading of SiW_{12}; however, further increase to 40% does not show any significant effect in acidic sites. This was also supported strongly from the surface area analysis that even though increasing the amount of SiW_{12} to 40%, the surface area almost remains the same as that of 30%. Hence, from the combine view point of surface area as well as acidity, 30% loading of SiW_{12} was considered to be appropriate for detailed characterization and catalytic evaluation, and $(SiW_{12})_3$/MCM-22 is recoded as SiW_{12}/MCM-22.

The N_2 adsorption-desorption isotherms and pore size distribution curve for MCM-22 and SiW_{12}/MCM-22 are shown in Fig. 1 a and b, respectively. The obtained isotherms (Fig. 1a) are of type IV with H4 hysteresis loop, exhibiting a regular trend of zeolites with the presence of micro as well as mesopores in the framework, which is also supported by the pore size distribution curve (Fig. 1b) (Thommes et al. 2015). The adsorption starting at very low P/Po value and extending up to higher relative pressure forms a virtually horizontal

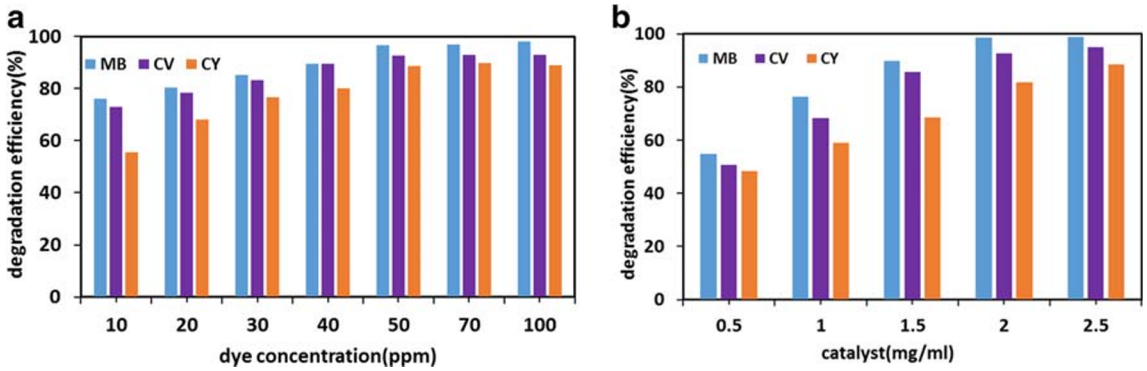

Fig. 6 (**a**) Effect of dye concentration (ppm); the concentration of MB, CV, and CY was varied from 10 to 100 ppm. (**b**) Effect of catalyst amount; the amount of catalyst SiW_{12}/MCM-22 was varied from 0.5 to 2.5 mg/mL; dye concentration, 100 ppm; reaction time, 60 min

plateau which is in good agreement with characteristic zeolitic nature of materials (Delitala et al. 2009). The isotherm curve obtained for SiW_{12}/MCM-22 is identical to that of MCM-22; however, comparative narrow hysteresis loop was observed which suggest the effective filling of SiW_{12} into the pores of MCM-22. This is also confirmed by the lower BET surface area of catalyst as compared to support.

FT-IR spectra of SiW_{12}, MCM-22, and SiW_{12}/MCM-22 are shown in Fig. 2. FT-IR of MCM-22 shows characteristic bands at 3441 cm^{-1}, 1635 cm^{-1}, 1226 cm^{-1}, 817 cm^{-1}, and 455 cm^{-1}. Band at 3441 is due to the O–H stretching of hydroxyl group of loosely bound water molecules. At 817 cm^{-1} and 1226 cm^{-1}, the bands are attributed to the symmetric and asymmetric stretching of T–O–T bond, respectively, where T = Si or Al. Stretching vibration corresponding to T–O, where the metal ion is bonded to four oxygen atoms, is observed at 455 cm^{-1} (Lonare et al. 2018). FT-IR of SiW_{12}/MCM-22 shows an additional band at 925 cm^{-1}, one of the characteristic bands for Keggin unit of SiW_{12} corresponding to asymmetric vibration of ($Si–O_a$). However, the other bands are not distinct due to their superimposition with that of support. Presence of this fingerprint band suggests that the primary of Keggin unit is intact even after impregnation on the support.

The XRD patterns of MCM-22 and SiW_{12}/MCM-22 (Fig. 3) show well-resolved characteristic peaks of MWW zeolitic structure in the range of 2θ 5–30° (Xing et al. 2015), suggesting that the crystalline framework of support remains unchanged even after the impregnation of SiW_{12}. However, less intense peaks are observed for catalyst which can be attributed to the inclusion of SiW_{12} inside MCM-22. Also, absence of the crystalline peaks of SiW_{12} indicates fine dispersion of active species into the support.

SEM images of MCM-22 and SiW_{12}/MCM-22 are shown in Fig. 4. From the images, morphology of MCM-22 appears to have very thin platelets which are interpenetrating each other and forms a lamellar particle. It is noteworthy that even after impregnation of SiW_{12}, there is no alteration as well as aggregation observed in the lamellar structure of MCM-22, indicating the stable morphology of the catalyst.

Table 2 Recycling results

Cycles	% Dye removal efficiency		
	MB	CV	CY
1	99	92	81
2	98	92	81
3	97	91	80
4	96	91	79

Catalytic degradation of dyes (MB, CV, and CY)

In the process of catalytic degradation of organic dyes by POMs, the dye chromophore can be damaged and broken down into smaller fragments or molecules that are less hazardous or non-polluting minor products (Ginimuge and Jyothi 2010). In the present work, the cationic dyes like MB, CV, and an azo dye CY were chosen as representative dyes to evaluate the degradation capability of the catalyst. The control experiments were first conducted to check the activity of original constituents of the catalysts, that is, only SiW_{12} and MCM-22. It is evident from Fig. 5 that the SiW_{12} as such shows the degradation efficiency nearly 16, 12, and 10% for MB, CV, and CY dyes, whereas MCM-22 shows much higher degradation efficiency 48, 46, and 40% for MB, CV, and CY dyes, respectively. The higher degradation efficiency of MCM-22 can be attributed to its high surface area (Table 1) as compared to bare SiW_{12}. The SiW_{12} exhibits surface area as low as < 10 $m^2\ g^{-1}$ with very good solubility in aqueous solvents (Hayashi and Moffat 1982) that makes it difficult to separate from reaction mixture, whereas the catalyst SiW_{12}/MCM-22 exhibits much better degradation efficiency. The large surface area of catalyst as shown in Table 1 enhances the accessibility of catalytic active sites that eventually explains the better dye degradation efficiency of the catalyst. The large surface area and pore diameter of the catalyst enable the greater adsorption of the dye molecules on to the catalyst and accessibility to

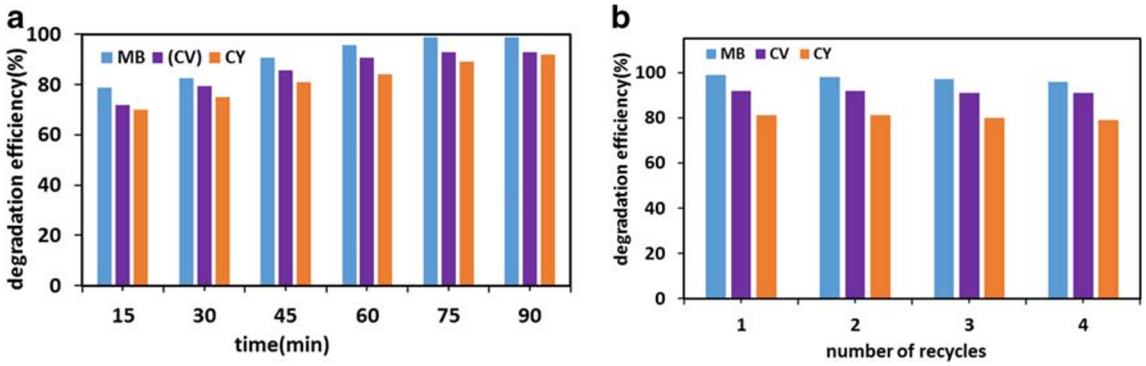

Fig. 7 (**a**) Effect of reaction time (minutes) and (**b**) recyclability of the catalysts

active cites and eventually desorption of degradation products. This explains the better performance of SiW_{12}/MCM-22 as compared to bare SiW_{12} and MCM-22 in dye degradation.

The concentration of all the dyes MB, CV, and CY, were varied from 10 to 100 ppm as depicted in Fig. 6a. Degradation efficiency increases for all the dyes with increase in concentration and then reaches saturation level which may be due to maximum surface coverage of the catalyst by these dyes. Hence all the experiments were carried out in 100 ppm dye concentration. The amount of catalyst was varied from 0.5 to 2.5 mg/ml (Fig. 6b). As the amount of catalyst increases, the degradation efficiency increases as expected. The maximum degradation efficiency as achieved at 2.5 mg/ml catalyst for multiple dyes.

The degradation efficacy of the catalyst was monitored at different time points from 15 to 90 min, and the maximum efficacy was achieved in 60 min itself (Fig. 7a). The trend was similar for all the dyes. Hence, the optimized conditions for multiple dye degradation are as follows: dye concentration, 100 ppm; amount of catalyst, 2 mg/ml; and reaction time 60 min. The catalyst was recycled for all the dye samples, and there was no significant decrease in degradation efficiency up to four cycles (Fig. 7b, Table 2). The recycling results depicts that there is no significant loss in dye removal efficiency up to four cycles with different dyes MB, CV, and CY. These results also indicate that the stability and activity of the catalyst were not perturbed with subsequent recycles. For cationic dyes MB and CV, catalyst shows better activity throughout all the experiments, but for an azo dye CY, the efficacy observed was slightly lower, as CY has residual negative charge at pH 7, and at this pH in water medium, all the experiments were carried out. This is further explained in the mechanism of the dye degradation in the following section.

Mechanism of dye degradation

The proposed oxidative degradation mechanism for multiple dyes MB, CV, and CY with MCM-22-supported POM, SiW_{12}, is schematically depicted in Fig. 8. Due to very high negative charge on $[SiW_{12}O_{40}]^{4-}$ anions, the adsorption mechanism of dye molecules might be predominantly attributed to an electrostatic interaction between the cationic MB and CV dyes with the negatively charged surface of SiW_{12}/MCM-22. Additionally, MCM-22 possesses quite large number of hydroxyl groups on the surface which also facilitates the adsorption of more dye molecules through hydrogen bonding. Once the dye molecules are adsorbed on the surface of the catalyst follows the catalytic degradation of dye molecules into smaller fragments due oxidation where in W in SiW_{12} has a role to play. The CY being a slightly negatively charged

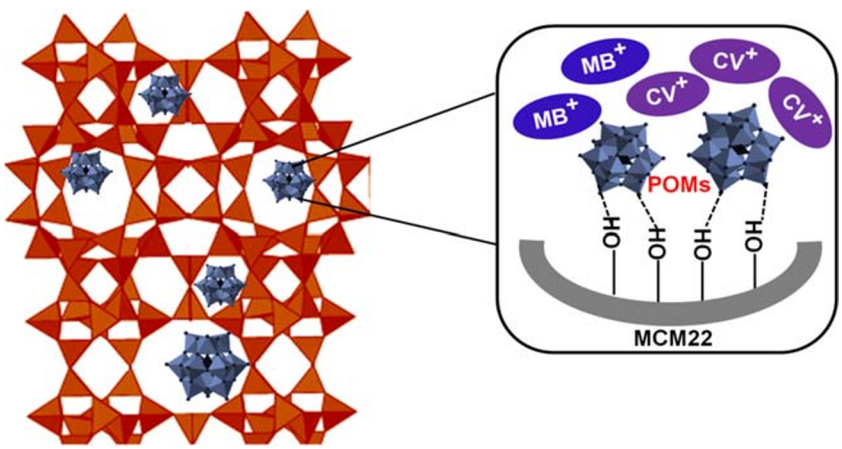

Fig. 8 Proposed mechanism of dye degradation over SiW_{12}/MCM-22 catalyst, electrostatic interaction with negatively charged surface of catalyst with cationic dyes followed by catalytic degradation of dyes by SiW_{12}

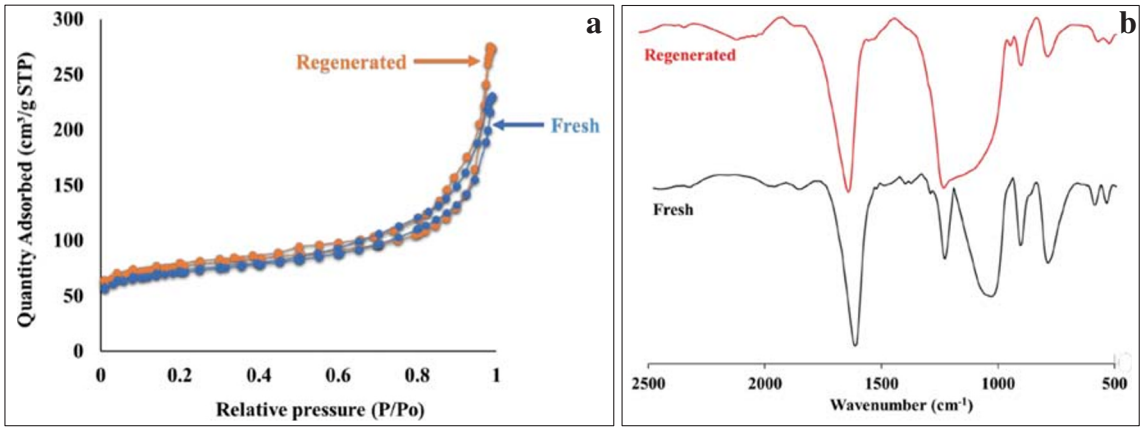

Fig. 9 (**a**) N_2 adsorption-desorption isotherms of fresh and regenerated catalyst and (**b**) FT-IR spectra of fresh and regenerated catalyst

dye molecule might experience slow adsorption on catalyst surface. Specifically, the degradation of MB is well documented in literature (Rauf et al. 2010; He et al. 2018). The oxidation of MB is initiated by demethylation resulting in degradation products of mono-demethylation, di-demethylation, tri-demethylation, and complete demethylation of nitrogen followed by ring opening. The similar results were also reported previously (Rauf et al. 2010, He et al. 2018).

Characterization of regenerated catalyst

To check sustainability of the synthesized catalyst, characterization for regenerated catalyst was performed by carrying out BET surface area and FT-IR analysis. The BET surface area of fresh and regenerated catalyst is 234 and 244 m^2/g, respectively, with parallel N_2 sorption isotherms curves (Fig. 9a), indicating no difference in the structure and nature of catalyst after the reaction. Also, the FT-IR spectra (Fig. 9b) of regenerated catalyst show the presence of all the characteristic bands with no shifting of values. This further confirms that there is no leaching as well as structural change of Keggin unit in the regenerated catalyst. Nevertheless, observed increase in the surface area as well as broadening of the band in FT-IR of regenerated catalyst may be attributed to the adsorption phenomenon that we explained in the mechanism section.

Conclusion

A catalyst, SiW_{12} anchored to MCM-22 was synthesized and characterized by various techniques like BET, FT-IR, XRD, and SEM. The lower BET surface area and pore volume of catalyst SiW_{12}/MCM-22, as compared to that of MCM-22, indicate the incorporation of active species SiW_{12}, inside the zeolitic pores of MCM-22. The uniform dispersion of SiW_{12} on MCM-22 was confirmed by XRD and also the lamellar morphology of MCM-22, and the catalyst was retained as observed in SEM. The catalyst was reported for degradation of cationic and azo dyes. The catalytic dye degradation of various organic dyes like MB and CV and CY was carried out. The comparison between the degradation efficiency of two dyes studies revealed that the catalytic oxidation in the aqueous solutions of cationic dyes like methylene blue (MB) and crystal violet (CV) could be carried out under the same operating conditions. The maximum degradation efficiency was found to be 95% and 90% for MB and CV, respectively, in 60 min, whereas the azo dye Chryosidine Y (CY) exhibits lower degradation efficiency in similar conditions that can be improved at higher time scale. The Chryosidine Y (CY) shows degradation efficiency of 84%. The catalyst was recycled for four cycles, and no significant decrease in activity was observed. Thus, the present material can be a promising catalyst for the management of toxic organic dyes and other pollutants in the coloured wastewater effluents.

Acknowledgement DP is thankful to Department of Chemistry, The Maharaja Sayajirao University of Baroda for all the facilities. AP and DP are thankful to the Department of Chemistry, The Maharaja Sayajirao University of Baroda, Vadodara, for BET measurements. VH and VB are thankful to Jain University, India, for providing facilities.

Authors' contributions Conceptualization: Anjali Patel and Varsha BrahmakhatriMethodology: Dhruvi Pithadia and Vinayak HegdeFormal analysis and investigation: Dhruvi Pithadia and Vinayak HegdeWriting - original draft preparation: Varsha Brahmakhatri, Dhruvi Pithadia, and Vinayak HegdeWriting - review and editing: Anjali PatelSupervision: Anjali Patel and Varsha Brahmakhatri

Data availability Not applicable.

Compliance with ethical standards

Competing interests The authors declare that they have no competing interests.

Ethical approval Not applicable.

Consent to participate Not applicable.

Consent to publish Not applicable.

References

Aragaw TA (2020) Recovery of iron hydroxides from electro-coagulated sludge for adsorption removals of dye wastewater: Adsorption capacity and adsorbent characteristics. Surfaces and Interfaces 18: 100439. https://doi.org/10.1016/j.surfin.2020.100439

Asolekar SR, Kalbar PP, Chaturvedi MKM, Maillacheruvu KY (2014) Rejuvenation of rivers and lakes in India: balancing societal priorities with technological possibilities. Elsevier Ltd.

Bamoharram FF, Niknezhad SH, Baharara J, Ayati A, Ebrahimi M, Heravi MM (2014) Amine-functionalized nanosilica-supported Dawson heteropolyacid: an eco-friendly and reusable photocatalyst for photodegradation of malachite green. J Nanostructure Chem 4. https://doi.org/10.1007/s40097-014-0088-z

Benkhaya S, M'rabet S, El Harfi A (2020) A review on classifications, recent synthesis and applications of textile dyes. Inorg Chem Commun 115:107891. https://doi.org/10.1016/j.inoche.2020.107891

Berradi M, Hsissou R, Khudhair M, Assouag M, Cherkaoui O, el Bachiri A, el Harfi A (2019) Textile finishing dyes and their impact on aquatic environs. Heliyon 5:e02711. https://doi.org/10.1016/j.heliyon.2019.e02711

Cao HL, Cai FY, Huang HB, Karadeniz B, Lü J (2017) Polyoxometalate-cucurbituril molecular solid as photocatalyst for dye degradation under visible light. Inorg Chem Commun 84:164–167. https://doi.org/10.1016/j.inoche.2017.08.021

Chen DM, Liu XH, Zhang NN, Liu CS, du M (2018) Immobilization of polyoxometalate in a cage-based metal–organic framework towards enhanced stability and highly effective dye degradation. Polyhedron 152:108–113. https://doi.org/10.1016/j.poly.2018.05.059

Dadashi Firouzjaei M, Akbari Afkhami F, Rabbani Esfahani M, Turner CH, Nejati S (2020) Experimental and molecular dynamics study on dye removal from water by a graphene oxide-copper-metal organic framework nanocomposite. J Water Process Eng 34:101180. https://doi.org/10.1016/j.jwpe.2020.101180

Delitala C, Alba MD, Becerro AI, Delpiano D, Meloni D, Musu E, Ferino I (2009) Synthesis of MCM-22 zeolites of different Si/Al ratio and their structural, morphological and textural characterisation. Microporous Mesoporous Mater 118:1–10. https://doi.org/10.1016/j.micromeso.2008.07.047

Fakhri H, Mahjoub AR, Aghayan H (2017) Effective removal of methylene blue and cerium by a novel pair set of heteropoly acids based functionalized graphene oxide: adsorption and photocatalytic study. Chem Eng Res Des 120:303–315. https://doi.org/10.1016/j.cherd.2017.02.030

Ginimuge PR, Jyothi SD (2010) Methylene blue: revisited. J Anaesthesiol Clin Pharmacol 4:517–520

Grabsi M, Zabat N, Khellaf N, Ismail F (2019) Synthesis of an environmental nano-polyoxometalate (α2P2W17CoO61)8− as catalyst for dyes degradation: a comparative study oxidation of indigoid and azo dyes. Environ Nanotechnology, Monit Manag 12:100269. https://doi.org/10.1016/j.enmm.2019.100269

Gürses A, Açıkyıldız M, Güneş K, Gürses MS (2016) "Dyes and pigments: their structure and properties" in SpringerBriefs in Green Chemistry for Sustainability. 13–29. https://doi.org/10.1007/978-3-319-33892-7

Han Y, Li H, Liu M, Sang Y, Liang C, Chen J (2016) Purification treatment of dyes wastewater with a novel micro-electrolysis reactor. Sep Purif Technol 170:241–247. https://doi.org/10.1016/j.seppur.2016.06.058

Hayashi H, Moffat JB (1982) The properties of heteropoly acids and the conversion of methanol to hydrocarbons. J Catal 77:473–484. https://doi.org/10.1016/0021-9517(82)90187-7

Hayat H, Mahmood Q, Pervez A, Bhatti ZA, Baig SA (2015) Comparative decolorization of dyes in textile wastewater using biological and chemical treatment. Sep Purif Technol 154:149–153. https://doi.org/10.1016/j.seppur.2015.09.025

He Y, Bin JD, Chen J et al (2018) Synthesis of MnO2 nanosheets on montmorillonite for oxidative degradation and adsorption of methylene blue. J Colloid Interface Sci 510:207–220. https://doi.org/10.1016/j.jcis.2017.09.066

Herrmann S, De Matteis L, de la Fuente JM et al (2017) Removal of multiple contaminants from water by polyoxometalate supported ionic liquid phases (POM-SILPs). Angew Chemie - Int Ed 56: 1667–1670. https://doi.org/10.1002/anie.201611072

Khumalo NP, Vilakati GD, Mhlanga SD, Kuvarega AT, Mamba BB, Li J, Dlamini DS (2019) Dual-functional ultrafiltration nano-enabled PSf/PVA membrane for the removal of Congo red dye. J Water Process Eng 31:100878. https://doi.org/10.1016/j.jwpe.2019.100878

Kumari S, Khan AA, Chowdhury A, Bhakta AK, Mekhalif Z, Hussain S (2020) Efficient and highly selective adsorption of cationic dyes and removal of ciprofloxacin antibiotic by surface modified nickel sulfide nanomaterials: Kinetics, isotherm and adsorption mechanism. Colloids Surfaces A Physicochem Eng Asp 586:124264. https://doi.org/10.1016/j.colsurfa.2019.124264

Lei P, Chen C (2005) Degradation of dye pollutants by immobilized polyoxometalate with H_2O_2 under visible-light irradiation. 39: 8466–8474. https://doi.org/10.1021/es050321g

Lellis B, Fávaro-Polonio CZ, Pamphile JA, Polonio JC (2019) Effects of textile dyes on health and the environment and bioremediation potential of living organisms. Biotechnol Res Innov 3:275–290. https://doi.org/10.1016/j.biori.2019.09.001

Li T, Li Q, Yan J, Li F (2014) Photocatalytic degradation of organic dyes by La3+/Ce 3+-H3PW12O40 under different light irradiation. Dalt Trans 43:9061–9069. https://doi.org/10.1039/c4dt00402g

Lonare MC, Gaikwad SN, Lonare C, et al (2018) Zeolite coated gold nano particles - a versatile nano catalyst. 5:192–214. ISSN NO: 2394-8442

Najafi M, Abbasi A, Masteri-Farahani M, Janczak J (2015) Two novel octamolybdate nanoclusters as catalysts for dye degradation by air under room conditions. Dalt Trans 44:6089–6097. https://doi.org/10.1039/c4dt03377a

Narkhede N, Singh S, Patel A (2015) Recent progress on supported polyoxometalates for biodiesel synthesis via esterification and transesterification. Green Chem 17:89–107. https://doi.org/10.1039/c4gc01743a

Patel A, Pathan S (2015) Springer briefs in molecular science polyoxomolybdates as green catalysts for aerobic oxidation

Rauf MA, Meetani MA, Khaleel A, Ahmed A (2010) Photocatalytic degradation of methylene blue using a mixed catalyst and product analysis by LC/MS. Chem Eng J 157:373–378. https://doi.org/10.1016/j.cej.2009.11.017

Singh S, Srivastava VC, Mall ID (2013) Mechanism of dye degradation during electrochemical treatment. J Phys Chem C 117:15229–15240. https://doi.org/10.1021/jp405289f

Sivakumar R, Thomas J, Yoon M (2012) Polyoxometalate-based molecular/nano composites: advances in environmental remediation by photocatalysis and biomimetic approaches to solar energy conversion. J Photochem Photobiol C Photochem Rev 13:277–298. https://doi.org/10.1016/j.jphotochemrev.2012.08.001

Thommes M, Kaneko K, Neimark AV, Olivier JP, Rodriguez-Reinoso F, Rouquerol J, Sing KSW (2015) Physisorption of gases, with special reference to the evaluation of surface area and pore size distribution (IUPAC Technical Report). Pure Appl Chem 87:1051–1069. https://doi.org/10.1515/pac-2014-1117

Tkaczyk A, Mitrowska K, Posyniak A (2020) Synthetic organic dyes as contaminants of the aquatic environment and their implications for ecosystems: a review. Sci Total Environ 717:137222. https://doi.org/10.1016/j.scitotenv.2020.137222

Vikrant K, Giri BS, Raza N, Roy K, Kim KH, Rai BN, Singh RS (2018) Recent advancements in bioremediation of dye: current status and challenges. Bioresour Technol 253:355–367. https://doi.org/10.1016/j.biortech.2018.01.029

Wang Q, Niu T, Jiao D, Bai Y, Zhong J, Li J, She H, Huang H (2017) Preparation of visible-light-driven BiOBr composites with heteropolyacids ($H_3PW_{12}O_{40}$) encapsulated by a zeolite for the photo-degradation of methyl orange. New J Chem 41:4322–4328. https://doi.org/10.1039/C7NJ00543A

Wang J, Zhang T, Mei Y, Pan B (2018) Treatment of reverse-osmosis concentrate of printing and dyeing wastewater by electro-oxidation process with controlled oxidation-reduction potential (ORP). Chemosphere 201:621–626. https://doi.org/10.1016/j.chemosphere.2018.03.051

Wu X, Luo B, Chen M, Chen F (2020) Tunable surface charge of Fe, Mn substituted polyoxometalates/hydrotalcites for efficient removal of multiple dyes. Appl Surf Sci 509:145344. https://doi.org/10.1016/j.apsusc.2020.145344

Xing E, Shi Y, Xie W, Zhang F, Mu X, Shu X (2015) Synthesis, characterization and application of MCM-22 zeolites via a conventional HMI route and temperature-controlled phase transfer hydrothermal synthesis. RSC Advances 5:8514–8522. https://doi.org/10.1039/C4RA11434E

Yaseen DA, Scholz M (2019) Textile dye wastewater characteristics and constituents of synthetic effluents: a critical review. Springer, Berlin Heidelberg

Zeng L, Xiao L, Long Y, Shi X (2018) Trichloroacetic acid-modulated synthesis of polyoxometalate@UiO-66 for selective adsorption of cationic dyes. J Colloid Interface Sci 516:274–283. https://doi.org/10.1016/j.jcis.2018.01.070